# Influence of Vegetation, Slope, and Lidar Sampling Angle on DEM Accuracy

**Jason Su and Edward Bork**

## Abstract

*Detailed GIS studies across spatially complex rangeland landscapes, including the Aspen Parkland of western Canada, require accurate digital elevation models (DEM). Following the interpolation of last return lidar (light detection and ranging) data into a DEM, a series of 256 reference plots, stratified by vegetation type, slope and lidar sensor sampling angle, were surveyed using a total laser station, differential GPS and 27 interconnected benchmarks to assess variation in DEM accuracy. Interpolation using Inverse Distance Weighting IDW resulted in lower mean error than other methods. Across the study area, overall signed error and RMSE were +0.02 m and 0.59 m, respectively. Signed errors indicated elevations were over-estimated in forest but under-estimated within meadow habitats. Increasing slope gradient increased vertical absolute errors and RMSE. In contrast, lidar sampling angle had little impact on measured error. These results have implications for the development and use of high-resolution DEM models derived from lidar data.*

## Introduction

Detailed geographic information system studies on complex rangeland landscapes, into aspects such as spatial plant ecology, animal behavior and soil hydrologic characteristics, require a highly accurate DEM. Although few technologies have been available in the past to generate DEMs of sufficient accuracy for use in detailed landscape applications, the use of lidar data may provide a suitable alternative. Previous research indicates accuracies of up to 15 cm RMSE may be obtained when imaging open, flat, and hard surfaces (Hodgson and Bresnahan, 2004; Pereira and Janssen, 1999). Under nearly ideal circumstances, Krabill *et al.* (1995) demonstrated a maximum detectable vertical resolution of 10 cm with lidar data when researching ice sheet thickness in the Arctic. Within landscapes where vegetation is structurally more complex, however, including those under shrub or forest cover, the error associated with lidar-derived DEMs tends to increase (Hodgson and Bresnahan, 2004; Reutebuch *et al.*, 2003). Despite this limitation, the vertical accuracy of many lidar systems remains relatively accurate compared to other remote sensing systems (e.g., videography and radar).

The total error associated with a lidar-derived DEM can be decomposed into various components. These generally include, in order of decreasing importance, the error from lidar system measurements, interpolation error, horizontal displacement error, and surveyor error (Hodgson and Bresnahan, 2004). Although it is common for the users of lidar data to adopt commercial ground-surface coordinate data as is (Reutebuch *et al.*, 2003), efforts should be made to identify, understand and where possible, reduce the error associated with DEM development. Despite this, limited research to date has quantified the influence of specific ground characteristics such as the type and density of vegetation (Narayanan and Guenther, 1998; Ni-Meister *et al.*, 2001), slope gradient (Bufton *et al.*, 1991) or other external factors such as off-nadir sampling angle (Tsutsui *et al.*, 1998) on the accuracy of a lidar-derived DEM. In general, few studies have evaluated the ability of lidar data to provide a DEM of high quality (e.g., low error) across all portions of spatially complex landscapes, as well as the role of external factors (i.e., equipment and environment) on DEM accuracy, necessitating further studies (Hodgson and Bresnahan, 2004).

Many rangeland landscapes, including the Aspen Parkland region of western Canada, consist of complex topography with frequent and rapid changes in slope gradient, aspect, and elevation (Ayad and Dix, 1964; Acton, 1965). These factors, in turn, interact prominently to alter the distribution of different plant communities across the landscape (Scheffler, 1976; Wheeler, 1976), as well as the frequency and magnitude of disturbances such as fire or grazing (Asamoah *et al.*, 2003). Moreover, meaningful ecological information for the management of land-use activities in these landscapes can only be obtained if the relative influence of topography and vegetation can be distinguished from one another. Within the Aspen Parkland environment, the use of existing DEM models with a coarse spatial resolution (i.e., >25 m) derived through manual or automated digitizing techniques from photographic sources, are clearly insufficient to accurately represent the rapidly changing local topography within these areas, where average relief is smaller than this resolution (e.g., 5 to 10 m).

The primary objective of this research was to evaluate the specific influence of external factors on the overall accuracy of a lidar-derived DEM, including environmental characteristics such as vegetation type and slope gradient, as well as equipment characteristics such as off-nadir angle during lidar sampling. This information will provide a greater understanding of the limitations in DEM accuracy relative to various intended end uses, and may provide direction on how DEM development can be improved. We also quantify the vertical error associated with horizontal displacement of the lidar and field DGPS systems where slope gradients exceed 0°. Finally, we assessed three different interpolators on the error associated with DEM development from raw lidar data for a complex Aspen Parkland landscape in central Alberta, Canada.

Agricultural, Food, and Nutritional Science Department, University of Alberta, 410 Agriculture/Forestry Center, Edmonton, Alberta, Canada T6G 2P5 (edward.bork@ualberta.ca).

Photogrammetric Engineering & Remote Sensing
Vol. 72, No. 11, November 2006, pp. 1265–1274.

0099-1112/06/7211–1265/$3.00/0

## Materials and Methods

### Study Area

This research was conducted at the University of Alberta Kinsella Research Station (53° 0′ N; 111°31′ W) located 150 km SE of Edmonton, Alberta, Canada, within the Aspen Parkland natural sub-region (Strong, 1992). The Research Station is 2,700 ha in size and has a general topography of rolling hills (i.e., knob and kettle terrain) with 5 to 10 m relief arising from its glacial moraine landform origin. The region has a temperate continental climate, with mean annual precipitation of 433 mm and 100 to 120 frost-free days (unpublished meteorological data). North-facing slopes are capable of supporting plant communities with greater moisture requirements such as shrublands and deciduous forest, while south-facing slopes support communities tolerant of drier conditions such as grasslands (Coupland, 1961; Wheeler, 1976). The most common soil type of the area is a Black Chernozem, although Dark Gray Chernozems and Eluviated Black Chernozems are present as well (Bailey and Wroe, 1974; Scheffler, 1976). Late summer dry matter herbage production from upland grassland, riparian meadow and forest vegetation averages 2062, 4862, and 1743 kg/ha, respectively (Asamoah *et al.*, 2003). The major vegetation types found across the study area and of interest in this investigation are as follows:

*Riparian Meadows*

Meadows are mesic to hygric habitats occupied by grass (*Poaceae* family) and grasslike species mostly of the genera *Carex* and *Juncus*. The primary environmental characteristic affecting meadow vegetation is the high water table during all or part of the year (Walker and Coupland, 1970). Two major types of wetlands occur at the Research Station, which include:

1. Saline riparian meadows dominated by sparsely vegetated salt grass (*Distichlis spicata* (L.) Greene), alkali grass (*Puccinellia nuttalliana* (Schultes) Hitchc.) and forbs. These areas border salt lakebeds and are associated with groundwater discharge.
2. Freshwater riparian meadows dominated by aquatic sedges (e.g., *Carex atherodes* Spreng.), tufted hairgrass (*Deschampsia caespitose* (L.) Beauv.), and marsh reedgrass (*Calamagrostis canadensis* (Michx.) Beauv.). These meadows occur at slightly greater elevations as groundwater recharge areas.

*Upland Grasslands*

Grasslands in this region were historically maintained by a combination of periodic fire (Wright and Bailey, 1982) coupled with grazing by ungulates including bison (*Bison bison*) (Campbell *et al.*, 1994). The two major upland grassland types at the Kinsella Research Station were described by Coupland (1961), and include:

1. Mixed prairie grassland dominated by western speargrass (*Stipa comata* Trin. & Rupr.) and northern wheatgrass (*Elymus lanceolatus* (Scribn. & J.G. Sm.) Gould). These dry grasslands are found on steep, south-facing slopes (>5°) and hilltops.
2. Fescue grassland dominated by plains rough fescue (*Festuca hallii* (Vasey) Piper) and western porcupine grass (*Stipa curtiseta* (A.S. Hitchc.) Barkworth). Although this grassland once covered much of the Aspen Parkland, most fescue grasslands have been ploughed for annual crop production or been overgrazed (Trottier, 1986). At the Kinsella Research Station, unbroken and moderately grazed fescue grassland remains abundant on mesic uplands with gentle slopes (<5°).

*Shrublands*

Upland shrublands are ecotonal between grassland and forest. Two major types of shrublands occur at the Research Station and include (after Wheeler, 1976):

1. Western snowberry (*Symphoricarpos occidentalis* Hook.).
2. Silverberry (*Elaeagnus commutata* Bernh. ex Rydb.).

Both snowberry and silverberry reproduce extensively by suckering from creeping underground roots, resulting in dense patches.

*Aspen Forest*

Forested areas at the Kinsella Research Station are represented by deciduous trembling aspen *(Populus tremuloides* Michx.) communities, with an understory of saskatoon (*Amelanchier alnifolia* (Nutt.) Nutt. ex M. Roemer), choke cherry (*Prunus virginiana* L.) and wild rose (*Rosa woodsii* Lindl) shrubs along with a well-developed herbaceous component. Aspen forest has expanded since European settlement (Bailey and Wroe, 1974; Scheffler, 1976), although recent outbreaks of forest tent caterpillars (*Malacosoma disstria*) and drought, coupled with prescribed burning have resulted in aspen stands of varied condition across the area. Young (5 to 30 years) and mature (30 to 60 years) aspen are both characterized by closed canopy stands of uniform tree age, height and diameter (Stelfox, 1995). In contrast, old and decadent aspen (>60 years) have undergone canopy break-up and subsequent understory release as well as the emergence of secondary young aspen and shrubs. As a result, aspen communities can generally be classified into either closed (young and mature) or semi-open (decadent) forest.

### Lidar Data Acquisition and Processing

Airborne scanning laser data were collected over the Kinsella Research Station using the Optech ALTM (Airborne Laser Terrain Mapper) 2025 system. The laser was flown 1,700 m above sea level, with an average above ground elevation of 1,005 m (ranging from 989 to 1,027 m) during the afternoon of 03 October 2000 during leaf-on conditions. Lidar sampling used an across-track scanning system with a Z-shaped target path. The wavelength and frequency of the laser pulse were 1.04 $\mu$m and 25 KHz, respectively. The mean return intensity was 42 percent and maximum off-nadir scanning angle 15°. Flight lines were approximately 500 m apart, with a total of 19 north-south lines covering the entire 2,700 ha area. The average laser footprint diameter was 0.3 m (0.071 $m^2$) directly below the aircraft, which increased to 0.31 m (0.075 $m^2$) at a distance of 250 m off-nadir. The average sampling interval was 1.5 m between footprints in the across-track direction and 1.3 m in the along-track (i.e., forward) direction. Final lidar data sampling densities across the area averaged 0.75 points/$m^2$, but ranged from 0.28 to 1.35 points/$m^2$.

Initial lidar data files consisted of two components including the real-time geo-corrected coordinates (UTM easting and northing, as well as *Z*-elevation) for each laser point on the ground (last return) and the top of the vegetation (first return). Individual elevations were calculated from the distances between the sensor and target. Distances were then derived from the speed of light (0.3 m/nanosecond) and length of time delay between the start and return pulse from the object being measured. Although sensor measurements can be affected by other radiance such as sunlight, Optech's instruments scan laser pulses within a preferred range of angles, and instruments are designed to operate in daylight (Optech, Incorporated, 2003).

The discontinuous last return ground lidar data points were subsequently interpolated into a continuous DEM surface to facilitate comparison of the lidar data to individual reference data points collected in July and August of 2001. Studies assessing interpolation methods have found differences, necessitating a comparison among them prior to use. Lloyd

and Atkinson (2002) used both cross-validation and a jack-knife procedure to assess the performance of ordinary kriging, kriging with trend, and inverse distance weighting (IDW) on the spatial interpolation of lidar data. The result was lower error using kriging with trend. While cross-validation is useful for identifying potential problems with DEM development (Lloyd and Atkinson, 2002), the jack-knife procedure has been identified as a superior method to compare interpolation methods for accuracy (Deutsch and Journel, 1998). We used the jack-knife validation procedure to select among splining, kriging and IDW interpolation methods for creating our final DEM. Four areas, each 4 $km^2$, were randomly selected from the entire lidar data set. Within those areas, 99.9 percent (total of 9,061,626 points) were randomly selected and used for DEM interpolation, while the remaining 0.1 percent (9,069 in total) were used for accuracy assessment and selection of the best interpolator: the latter involved comparison of interpolated and original raw lidar elevations. Finally, DEM interpolation errors were examined separately for those validation points in the landscape where slope gradient exceeded 15° to assess the potential influence of extremes in this environmental factor on interpolation error.

**Reference Data Sampling**

In order to evaluate DEM accuracy, a field survey was conducted in relation to the treatment variables, namely vegetation type, slope gradient, and off-nadir sampling angle. Due to limitations in the time availability for sampling reference data points, a preliminary power analysis (Thomas and Juanes, 1996) was conducted to determine how large a sample size was needed to detect treatment effects. Power is positively related to alpha level, the minimum treatment effect size, and the number of plots. Given that the main goal of this study was to detect treatment effects of slope gradient (including horizontal displacement), off-nadir sampling angle, and the four major vegetation types on lidar-derived DEM accuracy, our power analysis indicated approximately 250 reference points were required to achieve an effect size of 95 percent at an alpha of 5 percent.

A total of 260 reference data points were subsequently distributed across the study area landscape in a stratified random pattern. Points were stratified by vegetation type and slope gradient to ensure adequate sample sizes, but were randomly located around a series of benchmarks (BMs) distributed throughout the study area (Figure 1). Vegetation

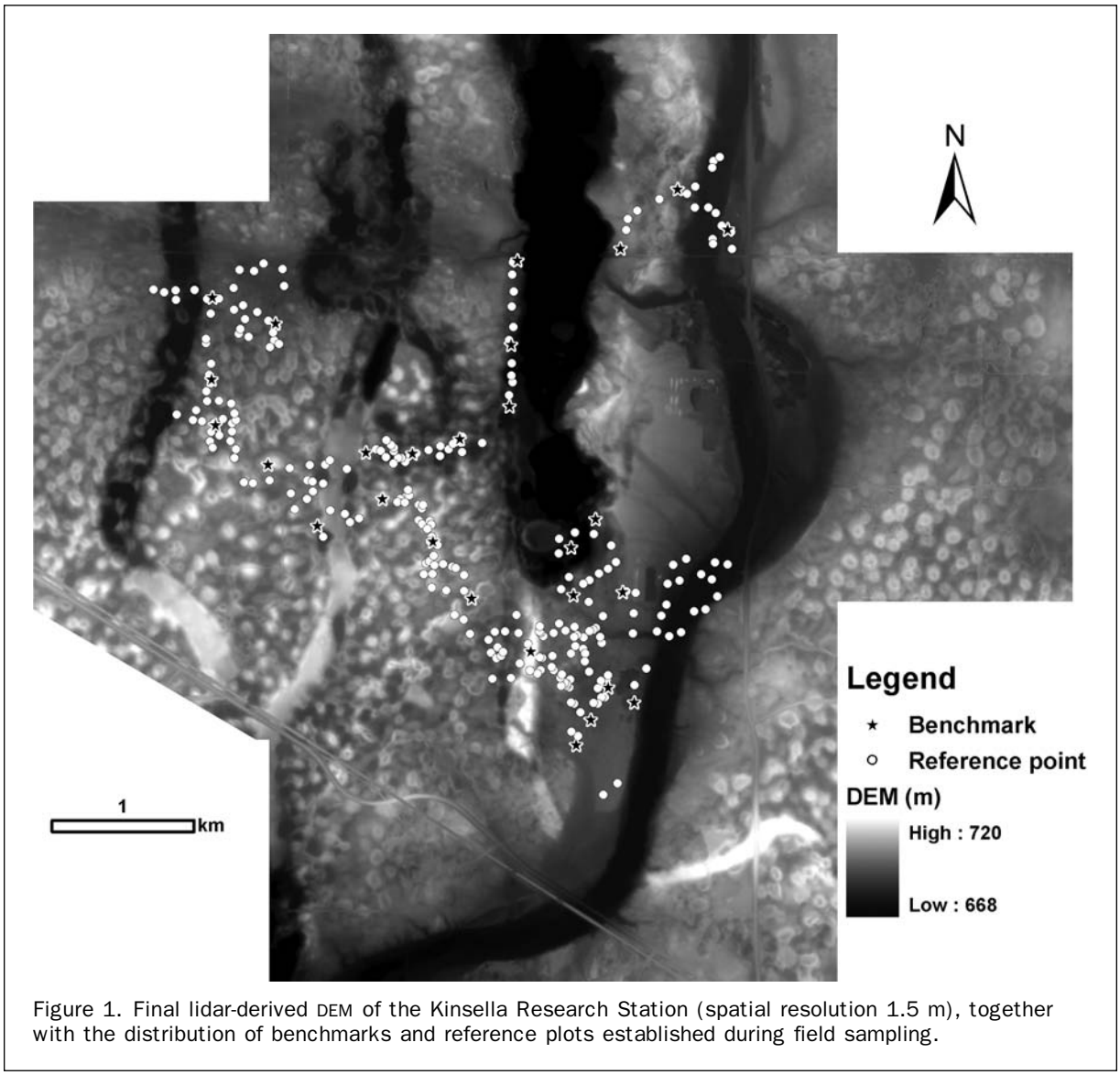


Figure 1. Final lidar-derived DEM of the Kinsella Research Station (spatial resolution 1.5 m), together with the distribution of benchmarks and reference plots established during field sampling.

types included the four general classes of upland grassland, deciduous forest, shrubland, and riparian meadow. However, these categories were further refined in the field to represent fescue and mixed prairie grasslands, closed and semi-open aspen forest, silverberry and western snowberry shrubland, as well as freshwater and saline riparian meadows. Slope gradients were stratified into low (<2°), moderate (2° to 5°), high (5° to 10°) and steep (>10°) slopes.

Although data points could not be stratified *a priori* by off-nadir angle because of difficulty in identifying these classes within the landscape prior to sampling, the widespread spatial distribution of points around benchmarks ensured all off-nadir categories were effectively sampled. Categories of off-nadir angle used for analysis were from 0° to 15°, in increments of 3°. At the mean elevation of the study area, the off-nadir sampling angles of 0°, 3°, 6°, 9°, 12°, and 15° coincided with the following sampling planimetric distances: 0 m, 52 m, 105 m, 158 m, 213 m, and 268 m.

The elevations of all reference plots were determined using a comprehensive sampling grid and a single known elevation benchmark located at the Research Station headquarters. The relative elevations of all reference points were measured using a Leica TCR 703 total laser station, and were linked using a grid of 27 interconnected benchmarks (BMs) set up across the study area (Figure 1). These BMs were used for transferring vertical elevations from one point to another using the block-station (Leica, 2000) transfer method (Figure 2: steps a and b). This method does not require the actual positional coordinates of the station, but instead facilitates calculation of the relative elevation of a target (e.g., BM), which is then passed on to calculate the relative elevation between two targets. Adjacent BMs were approximately 500 m apart ($n$ = 27 in total) to avoid exceeding the distance capability of the laser station. Each BM was positioned on top of a hill with a flat ground surface for convenient and accurate elevation transfer. Each time a new BM was established, back-sighting was used to validate the initial change in elevation (Figure 2: steps c through k), with BM No. 27 ultimately back-sighted to BM No. 1. Individual back-sight errors among all 27 benchmarks never exceeded 5 cm. Finally, all relative elevations were converted to absolute elevations using the lone geographical benchmark of known elevation at the headquarters, with BM No. 1 as the starting point: this same location was used to configure the lidar system. This sampling design ensured a high degree of accuracy within the absolute elevations of all BMs and their associated reference points.

Individual reference points were located between two-BMs and up to 250 m away from either one. At each of the 27 BMs, between 6 and 12 reference data points were

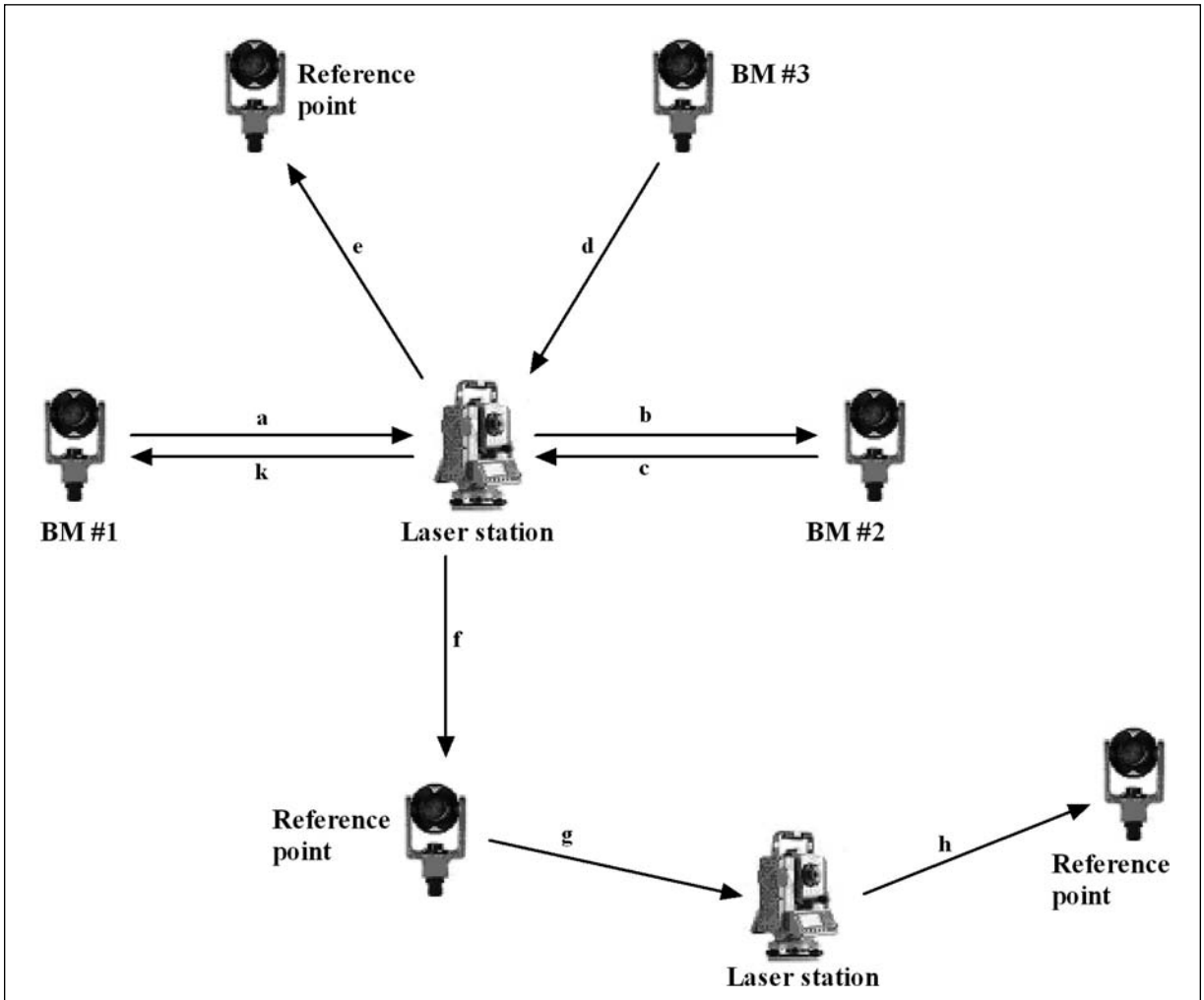


Figure 2. Total laser station working principle used for assessing DEM elevations within the 260 field plots. BM represents benchmark positions.

sampled using the free-station technique (Leica, 2000). This method uses a minimum of two and up to five known BMs to determine the elevation of a single reference point (Figure 2: steps a + c + d, then to e). By combining BMs, the free-station technique produced more reliable elevation measurements of individual reference points.

There were two additional situations in which the height-transfer method (Figure 2: steps f to g to h) was used to determine the ground elevation of a location. This included when the reference data points were more than 500 m away from the BMs, or more commonly, when reference data points were located inside closed aspen forest. In both situations, a transfer point was initially set up with the laser station situated between the transfer point and the targeted reference point in order to transfer the ground elevation from the transfer point to the target.

Corresponding positional coordinates ($X$ and $Y$ location) of each reference point were determined through the use of a differential-GPS (DGPS) system (mean horizontal accuracy = 0.53 m). These spatial coordinates were subsequently used to link the measured elevations derived from the laser station with those obtained from the lidar-derived DEM. Of the 260 original reference points, four were excluded from analysis because their horizontal accuracy based on the DGPS exceeded 1 m (raw data).

## Analysis

Three types of error have been commonly used to assess DEM accuracy, including mean signed error, absolute error, and RMSE. Mean signed error has been used previously to assess interpolation techniques (Lloyd and Atkinson, 2002) and overstory canopy closure effects (Reutebuch *et al.*, 2003) on the accuracy of a lidar-derived DEM, and has the benefit of indicating the directionality of errors. However, absolute error and RMSE have also been used to assess DEM accuracy (Clark *et al.*, 2004). Hodgson and Bresnahan (2004) used mean signed error, absolute error, and RMSE in their assessment of a lidar-derived DEM. Similar to the latter study, mean signed errors were used in our analysis to identify the tendency for under- or over-estimation of elevations relative to specific treatment classes (i.e., vegetation type, slope, and sampling angle). Absolute errors were used to identify trends in DEM accuracy under extreme environmental conditions, for example, the top five absolute errors within a vegetation type. In the last step, the RMSE was used to determine the overall mean elevation accuracy of the lidar-derived DEM for all treatments.

Prior to testing the impact of treatment variables on DEM accuracy, the three interpolation methods used were compared and evaluated to facilitate selection of one interpolation method for the remaining analysis. Interpolation error using the jack-knife procedure was assessed based on values of mean signed error and RMSE (Equation 1). RMSE was calculated using the formula:

$$RMSE_{Interpolation} = \sqrt{\frac{\sum_{i=1}^{n}\left(Z_i^{interp} - Z_i^{LIDAR}\right)^2}{n}} \quad (1)$$

where $Z_i^{interp}$ and $Z_i^{LIDAR}$ are the interpolated and lidar-derived elevations at cell $i$, and $n$ is the total number of points used for interpolation. Interpolation mean signed error and RMSE were examined for all validation lidar points, as well as specifically those validation points with a slope gradient greater than 15°. Both analyses indicated that the IDW method generally resulted in smaller interpolation errors compared to the other methods, with kriging resulting in greater errors relative to splining (Su, 2004). RMSE values for kriging and splining were 0.02 m larger, on average, than the IDW method. When slope gradients exceeded 15°, the kriging and splining interpolation methods still produced greater errors (by 0.01 m) relative to the IDW method. Based on these preliminary findings, the IDW interpolation method was applied to all the lidar data to create a DEM with spatial resolution of 1.5 m (Figure 1).

To assess the affect of specific treatment variables on DEM error across the study area, modelled elevations were extracted from the IDW interpolated surface for all 256 reference points and subsequently compared to the surveyed elevations for those same points. Differences in elevation were used to test the influence of slope gradient, off-nadir sampling angle, and vegetation type (Jensen, 2000), as well as horizontal accuracy of the lidar and field GPS systems, on the resulting accuracy of the lidar-derived DEM.

All reference points were classified into four slope gradient classes, with the corresponding sample sizes among the 0° to 2°, 2° to 5°, 5° to 10° and >10° slope classes ranging from 125 to 42, respectively, likely in proportion to their abundance in the landscape. Estimated lidar-derived elevations were compared to their corresponding reference data within each slope class. Mean signed error was again used to identify tendencies of elevation over- or under-estimation within slope classes. Next, the error associated with various off-nadir angles within individual slope categories was calculated to assess the interaction between these factors. The mean of the top five signed and absolute errors, along with their corresponding off-nadir angles, were also calculated to identify whether DEM errors were affected by extremes in slope. As a last step, the RMSE was used to determine the overall mean elevation accuracy of the lidar-derived DEM within each slope class (Equation 2). RMSE was determined as follows:

$$RMSE_{total,i} = \sqrt{\frac{\sum_{j=1}^{n}\left(Z_{i,j}^{reference} - Z_{i,j}^{\text{int } erp}\right)^2}{n}} \quad (2)$$

where $RMSE_{total,i}$ is the overall mean error within slope class $i$ and $i$ = 1 (0° to 2°), 2 (2° to 5°), 3 (5° to 10 °), and 4 (>10 °), $n$ is the total number of observations in slope class $i$, $Z_j^{reference}$ is an elevation measured from a reference point at location $j$, and $Z_j^{\text{int } erp}$ is the same as in Equation 1.

Apart from $X$ and $Y$ coordinates, elevation, and intensity data, the raw lidar data provided specific flight-line information during sampling. This information was used to derive the specific flightline from which the lidar data originated for each reference point. In order to assess off-nadir angle effects, lidar data points along individual flightlines were first converted to continuous lines (average swath interval of approximately 500 m). Lines were then buffered with off-nadir planimetric distances of 52 m, 105 m, 158 m, or 213 m (corresponding to off-nadir sampling angles of 3°, 6°, 9°, and 12°, respectively). The final class was greater than 213 m, and included all points beyond that but before the mid-point between successive flightlines. Reference point sample sizes per class varied from 32 to 63. In order to test the effect of off-nadir angle on DEM accuracy, the elevations of reference points within each angle class (0° to 3°, 3° to 6°, 6° to 9°, 9° to 12°, and 12° to 15°) were compared to the lidar-derived elevations for the same locations. Mean signed, absolute, and RMSE errors were estimated for each of the five off-nadir angle categories. Given that Hodgson and Bresnahan (2004) predicted observable errors on steep slopes (e.g., >25°) to be significantly larger than those on flat areas or low slopes (<4°), the mean slope gradient within each off-nadir class was also calculated to determine whether any errors present were associated with

slope gradient. The mean of the top five signed and absolute off-nadir errors were again determined.

Elevations from the lidar-derived DEM and reference points were compared within each of the four general vegetation classes, including upland grasslands, shrublands, deciduous forest, and lowland meadows. The comparatively smaller number of reference points in lowland meadow ($n$ = 27) was due to the limited area of that vegetation type within the study area (about 4 percent by area). An analysis similar to that for slope gradient and off-nadir angle was conducted for vegetation. In addition, where DEM error was found to be impacted by the four general vegetation types, this analysis was repeated using the eight, more detailed vegetation types, thereby enabling a more discrete comparison to be made between plant community types within different habitats.

The last step in our analysis was to examine the degree of modeled DEM error that may have arisen from horizontal displacement through the DGPS (linking the ground data to lidar data), as Hodgson and Bresnahan (2004) found horizontal displacement combined with slope to contribute to vertical error. In the present study, we postulated that both lidar sampling and the field DGPS survey system created horizontal positional errors, thereby adding vertical error. The vertical error associated with horizontal displacement of the lidar system was estimated using Equation 3 (modified from Equation 6 of Hodgson and Bresnahan, 2004). Similarly, the vertical error associated with horizontal displacement of the field DGPS system was calculated from Equation 4. Combining these equations resulted in a method (Equation 5) to estimate the vertical errors of lidar sampling and the field DGPS survey system as a result of horizontal displacement.

$$RMSE^{LIDAR}_{Horizontal,Slope} = \left(0.689282633 * Tan\left(\overline{Slope}\right) * RMSE^{LIDAR\ DGPS}_{Horizontal}\right) + \left(0.006194908 * RMSE^{LIDAR\ DGPS}_{Horizontal} * \sigma_{Slope}\right) \quad (3)$$

$$RMSE^{Field\ DGPS}_{Horizontal,Slope} = \left(0.689282633 * Tan\left(\overline{Slope}\right) * RMSE^{Field\ DGPS}_{Horizontal}\right) + \left(0.006194908 * RMSE^{Field\ DGPS}_{Horizontal} * \sigma_{Slope}\right) \quad (4)$$

$$RMSE^{Slope}_{Horizontal} = \left(0.689282633 * Tan\left(\overline{Slope}\right) * \left(RMSE^{Field\ DGPS}_{Horizontal} + RMSE^{LIDAR\ DGPS}_{Horizontal}\right)\right) + \left(0.006194908 * \left(RMSE^{Field\ DGPS}_{Horizontal} + RMSE^{LIDAR\ DGPS}_{Horizontal}\right)\right) * \sigma_{Slope} \quad (5)$$

The horizontal RMSE arising from the field DGPS was calculated using Equation 6:

$$RMSE^{Field\ DGPS}_{Horizontal} = \sqrt{\frac{\sum_{i=1}^{n} \alpha_i * \alpha_i}{n}} = 0.56 \text{ m} \quad (6)$$

where $\alpha$ is the field observed DGPS horizontal accuracy (m) at point $i$, and $n$ is the number of measurements inside that observed class. The mean slope gradient of the reference data points in our study area was 4.33° (+/−5.45°) and lidar horizontal RMSE $\left(RMSE^{LIDAR\ DGPS}_{Horizontal}\right)$ of 1 m.

## Results and Discussion

### DEM Interpolation Accuracy

The results of our study indicated that IDW created an interpolation surface with less overall error compared to kriging (Table 1). This contrasts the findings of Lloyd and Atkinson (2002), who examined a land area with similar slope gradients (2° to 4°) to that investigated here, and used similar jack-knife validation techniques and applied similar interpolation methods, including kriging and IDW.

Differences in interpolated DEM accuracy have been associated with variation in the density of lidar sampling points, with greater densities increasing accuracy (Gong *et al.*, 2000; Raber, 2003), and may account for the discrepancy between the current and previous studies. Our research used lidar data with a mean density of 0.75 points/m$^2$ to select an interpolation method. In comparison, the jack-knife validation applied by Lloyd and Atkinson (2002) used either 50 percent, 25 percent, or 5 percent of the total raw data (139,694 points at 250,000 m$^2$ area) for interpolation, which corresponded to lidar densities of 0.28, 0.14, and 0.03 points/m$^2$. Densities in the latter study were therefore well below our density and might explain why IDW was more effective in our investigation. In fact, Lloyd and Atkinson (2002) recommended simpler interpolation approaches be used where the sample spacing was small, similar to the situation in our study.

### Slope Gradient

Previous studies have found elevation errors to be greater in areas of steeper slopes when using the GPM (Gestalt Photomapper), manual profiler, or modeled statistical methods (Chang and Tsai, 1991; Bolstad and Stowe, 1994; Gao, 1995; Gong *et al.*, 2000). Hodgson *et al.* (2003) also identified a significant monotonic relationship between the mean absolute elevation error and increasing slope for a lidar-derived DEM. In our study, mean signed error did not increase proportionally to slope gradient (Figure 3a), with the largest signed error associated with intermediate slopes between 2° to 5°. How-

TABLE 1. DESCRIPTIVE STATISTICS OF INTERPOLATION ERRORS OBTAINED BY DEDUCTING LIDAR ELEVATIONS FROM INTERPOLATED DEM ELEVATIONS. DATA CONSIST OF EITHER ALL THOSE POINTS USED FOR ESTIMATION (0.1 PERCENT), OR ONLY THOSE WITH A SLOPE GRADIENT GREATER THAN 15°

| | All Data Used for Interpolation | | | Only Data with Slopes >15° | | |
|---|---|---|---|---|---|---|
| | Kriging | Splining | IDW | Kriging | Splining | IDW |
| *N* | 9069 | 9069 | 9069 | 335 | 335 | 335 |
| Range of error (m) | 1.856 | 3.158 | 1.568 | 1.788 | 1.455 | 1.568 |
| Minimum signed error (m) | −0.657 | −2.326 | −0.601 | −0.588 | −0.623 | −0.601 |
| Maximum signed error (m) | 1.199 | 0.832 | 0.967 | 1.199 | 0.832 | 0.967 |
| Mean signed error (m) | 0.0035 | 0.0028 | 0.0028 | −0.0063 | −0.0060 | 0.0018 |
| RMSE (m) | 0.133 | 0.140 | 0.116 | 0.200 | 0.205 | 0.186 |
| Error skewness | 0.1181 | −0.5687 | 0.0001 | 0.3880 | −0.0004 | 0.2385 |

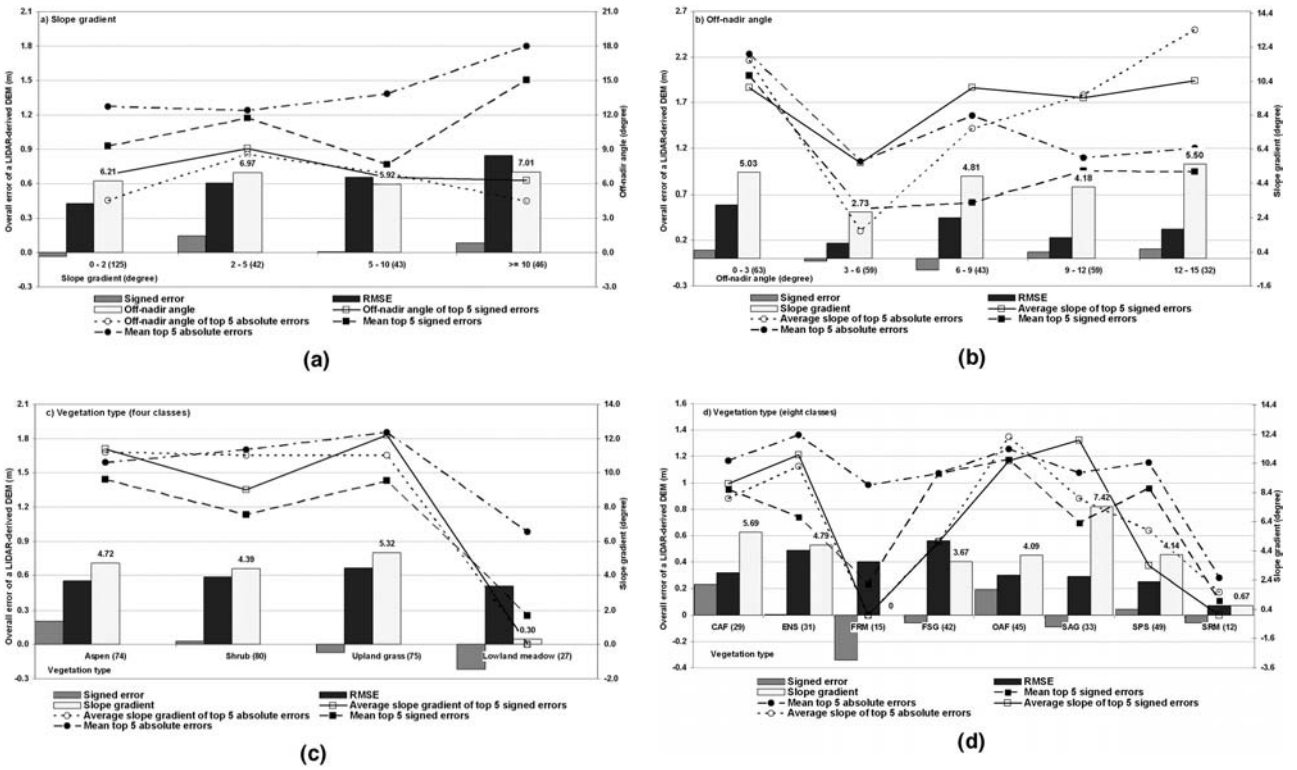


Figure 3. Overall lidar-derived DEM errors from (a) slope gradient, (b) off-nadir angle, and vegetation type for (c) four vegetation classes, and (d) eight vegetation classes. Digits in parentheses are the number of reference data points of that class. CAF = closed forest, ENS = silverberry shrublands, FRM = freshwater meadows, FSG = fescue grassland, OAF = semi-open forest, SAG = mixed prairie grassland, SPS = western snowberry shrublands, and SRM = saline meadows.

ever, further examination of the mean top five signed errors indicated that where slopes were less than 10°, the error associated with slope was positively related to its corresponding off-nadir angle (Figure 3a). The magnitude of the signed error associated with slope might therefore be contributions from, (a) extreme slope-based errors, which in turn, were magnified by high off-nadir angles, or (b) random error canceling, which created smaller mean signed errors when slopes exceeded 5°. The insignificant correlation between the mean top five absolute errors and their corresponding off-nadir angles supported the notion that the DEM errors associated with extreme slope gradients were not caused by their accompanying off-nadir angles, but rather random error canceling. Finally, RMSE values indicated the lidar-derived DEM accuracy generally decreased as slope gradient increased: the RMSE at slopes over 10° was twice that found when slopes were less than 2°. This finding was similar to Hodgson and Bresnahan (2004), who observed errors on slopes of 25° to be twice that found on relatively flat areas.

### Off-nadir Sampling Angle

Signed errors and RMSEs were generally greater when lidar data were collected close to nadir (less than 3°) relative to those sampled in angle classes further away from the central flightline (Figure 3b). However, this pattern may be attributed to the presence of extreme errors. The mean top five signed errors near nadir were 23 times larger than their corresponding overall signed errors. Moreover, extreme errors were accompanied by high (>10°) slope gradients, which may also have contributed to the observed elevation errors. The smallest RMSE occurred in the off-nadir class of 3° to 6°, which notably also had the lowest mean slope gradient. In contrast, two of the three angle classes with the top five absolute errors (0° to 3°, 9° to 12° and 12° to 15° off-nadir) were associated with slopes greater than 8° (Figure 3b), suggesting any minor differences in DEM error across off-nadir angles may be the result of differences in slope rather than sampling location.

### Vegetation Type

In identifying a tendency to under- or over-estimate elevations, the mean signed errors in Figure 3c show that elevations within aspen forest were over-estimated (+0.20 m) while those in lowland meadows were under-estimated (–0.22 m). Examination of the eight detailed classes of vegetation revealed a strong tendency to over-estimate elevations in both closed and semi-open aspen forest (Figure 3d). Ni-Meister *et al.* (2001) indicate that leaf orientation and shape contribute to the change of foliage profile and influenced lidar data accuracy. The leaves of aspen and associated understory forbs (i.e., broadleaf dicots) are oval-shaped and usually horizontally oriented. This kind of vegetation can attenuate laser beam irradiance passing through the canopy more readily, and promptly reflect signals back to the lidar sensor. As a result, many lidar last return signals may originate from the forest canopy or understory vegetation rather than true ground, particularly with a small footprint lidar system.

Over-estimations of elevation in shrub and forest vegetation have been found in other studies (Reutebuch *et al.*, 2003; Hodgson *et al.*, 2003). For example, Reutebuch *et al.* (2003) had a mean signed error of 0.31 m within a lidar-derived

DEM for unlogged forests. This is similar to our situation (mean signed error = 0.23 m) in which closed aspen forests were uncut and in leaf-on conditions. In addition, Reutebuch *et al.* (2003) found no significant effects of local canopy cover under a conifer forest (mean signed error difference of 0.15 m between heavily thinned, lightly thinned and the uncut class), which is consistent with our findings when closed and semi-open aspen forest were compared (mean signed error difference of 0.05 m).

We also noted that the average slope gradient of the top five signed errors in aspen forest was 11° (Figure 3c), which included 9° and 11° in closed and semi-open aspen forests (Figure 3d), respectively. As a result, the previously documented affects of slope may also contribute to the over-estimation of elevations within aspen forest. Although upland grasslands had similar slope extremes as the aspen forest, the shorter vegetation height in grasslands may limit the compound effects of slope and vegetation.

Both Hodgson and Bresnahan (2004), and Hodgson *et al.* (2003) found signed elevation errors were high in the shrub (i.e., shrub) vegetation category compared with other vegetation. However, in our study the two shrubland vegetation types, particularly silverberry, had the lowest signed error among all vegetation types. This finding may be due to the timing of lidar data collection in early October. Although the aspen overstory remained in leaf-on conditions and lowland meadows typically contained abundant senescent plant residue during lidar sampling at this time, many shrubs including silverberry had experienced significant leaf loss, potentially increasing the likelihood of the lidar signal originating from nearer the ground surface. Additionally, because the shrub vegetation type was consistently situated between forest and grassland areas as an ecotonal plant community, it is possible that the associated interpolation of the over-estimated elevations under forest and the under-estimated elevations in grassland actually combined to map ground elevations more accurately in these transitional landscape areas.

Grasslands at the Research Station were dominated by monocots with vertical-oriented leaves, which may explain the tendency for elevations in this type to be under-estimated. This canopy architecture could cause repeated bouncing back and forth of incoming lidar signals within the grass canopy, which may have delayed the lidar return signal emanating from grasslands. However, the high-signed errors associated with lowland meadows, particularly freshwater riparian meadows, may also be readily explained by the micro-topography and timing of data collection. Freshwater riparian meadows were typically flooded in spring and grazed by cattle during summer. The resulting micro-topography of this habitat was not a flat surface, but rather numerous *pits* created by cattle hooves stepping in soft soil. Therefore, it would not be unusual for elevation changes up to 30 cm to occur in as little as 10 cm horizontal distance, potentially introducing an error of 0.3 m even though the overall topographic slope gradient remained unchanged. Due to high moisture availability, riparian meadows also tended to consist of relatively tall grasses (mean height = 0.61 m), with grazing often resulting in small, heavily utilized patches where vegetation was much shorter. This unevenness may also have contributed to the confusion in modeling ground elevations from lidar returns.

Among all vegetation types, RMSE values were greatest for upland grasslands and least for lowland meadows (Figure 3c). One possible explanation for this pattern was that the upland grasslands were affected more significantly by steeper slope gradients. However, examination of absolute errors among the eight vegetation types (Figure 3d) indicated the mixed prairie upland grassland had a high slope gradient but comparatively low RMSE. In contrast, the other upland grassland type (fescue) had comparatively low slope gradients but high RMSE values. Thus, slope gradient was discounted as the primary factor influencing RMSE and the observed lidar-derived DEM accuracy. Instead, background noise within the lidar signals might have contributed to the high RMSE (Weltz *et al.*, 1994) observed in fescue grasslands. Unlike either of the upland grasslands, saline riparian meadows were situated in flat topographic depressions and had comparatively sparse, low-stature vegetation at the time of lidar sampling. Thus, few extreme slope values were observed, and coupled with the low plant cover and limited associated grazing activity, likely account for the low RMSE in this vegetation type. Notably, in the studies of Reutebuch *et al.* (2003) and Hodgson *et al.* (2003), as well as that of our study, none of the open grasslands had an ideal signed error of 0 m, potentially indicative of a bias contributed by the GPS control during lidar sampling.

In addition to canopy structure influences on laser responses and corresponding DEM accuracy, the inherent characteristics of small footprint laser systems limit their application in dense and complex forest areas. Hofton *et al.* (2002) mapped 800 $km^2$ of Costa Rica using 25 m diameter footprints as part of the pre-launch activities of the Vegetation Canopy lidar (VCL) Mission. Crossover analysis using laser shots, whose recorded waveforms contained more than 50 percent of the total returned energy within their lowest reflections, found elevation accuracy to be more than 50 percent greater compared to a corresponding small footprint lidar system. In our study, the small footprint lidar system only recorded first and/or last returns, making it difficult to determine whether or not a particular laser shot has fully penetrated the canopy to the ground.

In contrast, large-footprint (>10 m diameter) lidar systems digitise the entire return signal (e.g., in approximately 30 cm vertical bins), thereby providing a vertical distribution profile of intercepted surfaces (or "waveform") from the top of the canopy to the ground. With a large-footprint lidar, laser energy consistently reaches the ground even in dense forests. The difficulty of penetrating complex forest canopies will promote the use of large footprint waveform laser altimetry to measure sub-canopy topography (Hofton *et al.*, 2002). This process may therefore help overcome the influence of woodland vegetation on DEM accuracy, although areas with rapid changes in relief such as those examined here may impose other limitations on the maximum size of footprint that can be successfully used. Conversely, in northern hardwood forests, a small footprint lidar may be more useful and economical for DEM development when sampling is performed either in the fall after vegetation is dormant, or in the spring prior to leaf-out of deciduous trees and shrubs, and the development of new herbaceous growth. Alternatively, timing lidar sampling to coincide with the removal of plant residue through grazing or the use of prescribed fire, both common activities at the Research Station, may also increase DEM accuracy.

#### Horizontal Displacement

Previous studies have indicated that horizontal displacement can be a major contributor to vertical DEM error (Hodgson and Bresnahan, 2004). The vertical RMSE caused by horizontal displacement associated with the lidar and field DGPS systems used in this study were 0.08 m and 0.05 m, respectively, creating a total vertical RMSE of 0.13 m. The 0.08 m vertical error arising from horizontal (lidar) displacement was similar to the lidar system vertical error of 0.06 m identified by Hodgson and Bresnahan (2004). However, as noted earlier, slope gradients greater than 10° resulted in the greatest RMSE of 0.28 m. Increasing vertical

RMSE with steeper slopes in our study further supported the findings of Hodgson *et al.* (2003), who identified a significant monotonic relationship between mean absolute elevation error and increasing slope for a lidar-derived DEM. In the current study, the magnitude of vertical RMSE created by horizontal displacement was relatively consistent (approximately 0.15 m) among different categories of off-nadir sampling angles.

When compared across the four and eight vegetation types, lowland meadows including both fresh and saline, had the smallest vertical error (0.02 m) associated with its horizontal displacement, likely because of negligible slope effects. Among the aspen forest, shrubland, and upland grassland vegetation types, RMSE values were more similar, probably because they had comparable slope gradients. However, even among these types, some differences were apparent. Upland grasslands had greater vertical RMSE (0.18 m) than forest (0.17 m) and shrubland (0.14 m) areas. Notably, upland grasslands had a mean slope gradient among reference plots of 5.32°, greater than that of both forest (4.72°) and shrubland (4.39°) vegetation types. Furthermore, within upland grasslands, the mixed prairie type had the greatest vertical RMSE, likely due to its mean slope of 7.42°, suggesting slope combined with vegetation type to influence vertical accuracy in this investigation.

## Conclusions and Management Implications

This study found that small footprint lidar data can be used to effectively model landscape DEM properties within the Aspen Parkland of western Canada, despite having high topographic complexity and diverse vegetation. Furthermore, IDW was found to be a simpler and more accurate interpolation method than kriging for DEM development, likely due to the high density of lidar data points available (>0.75 points/$m^2$) in our study. However, accuracy of our lidar-derived DEM also varied spatially across the landscape, primarily in response to vegetation type, slope gradient, and horizontal displacement of the DGPS in the lidar system. Greater signed errors were associated with forest and lowland meadow vegetation types, as opposed to shrublands or upland grasslands. Forested vegetation resulted in over-estimated elevations, potentially due to interference from the understory on the lidar return signal. In contrast, modelled elevations in meadows were under-estimated. Slope gradient was also an important variable effecting DEM accuracy, with steeper slopes resulting in increased DEM error. The RMSE attributed to slope was also partly attributed to horizontal displacement of the DGPS and the lidar system. In contrast, sampling angle of the lidar system (to a maximum of 15°) had relatively little impact on DEM accuracy, although errors due to extremes in slope gradient tended to be exacerbated at the largest sampling angles examined.

Overall, the lidar-derived DEM developed in this investigation had a mean signed error of +0.02 m and RMSE of 0.59 m, based on the reference data collected. This level of accuracy is more than sufficient for landscape-based management activities such as undertaking rangeland inventory, plant community monitoring, and the development of basic grazing or prescribed burning plans. However, the suitability of this level of accuracy will also be determined by the ultimate intended use of the DEM. For example, detailed spatial scientific studies on animal grazing behavior or plant community ecology in this type of variable landscape may require a greater degree of confidence in the location of specific habitats relative to various positions across the landscape, particularly those in ecotonal transitions. In this situation, DEM error values of a half-meter or more may limit the utility of these spatial data for detailed landscape-based ecological studies.

Based on the results of this research, the greatest source of error within the lidar-derived DEM was that of vegetation. In order to limit the influence of vegetation on the resulting DEM, steps should be taken to sample these Parkland landscapes when interference from vegetation is minimal. For example, sampling during early spring or late fall may decrease the influence of taller-stature vegetation and increase DEM accuracy. Similarly, sampling with lidar systems could be timed to coincide with the removal of vegetation, either through grazing, or more likely, prescribed burning. The latter procedure would be preferable as it would remove the majority of above-ground biomass and help ensure that lidar signals emanate from ground surfaces rather than vegetation canopies.

Unlike vegetation, the influence of slope gradient on DEM error may be more problematic to mitigate because slopes cannot be modified prior to sampling. Nevertheless, our results do suggest that in order to minimize DEM errors associated with high slope gradients, off nadir sampling angles should be kept less than 15° (i.e., flightlines should be closely spaced) and once again, vegetation influences should be minimized to avoid interactions of the latter (i.e., particularly forest communities) with steep slopes. Finally, our results also suggest that the relative accuracy of DEM-based landscape data should be tempered by an understanding of local slope patterns. Combined with an understanding of vegetation conditions at the time of sampling, this information may be used to collectively minimize error within a lidar-derived DEM.

## Acknowledgments

Financial support for this study was provided by the University of Alberta, the Kinsella Research Station, Butler Survey Supplies, the Alberta Research Council, and a FS Chia scholarship to Jason Su. We thank Dr. Evelyn Merrill, Dr. Peter Crown, Dr. Yuguang Bai, and Dr. Ed Korpela, as well as Dr. Merchant and three anonymous reviewers for their helpful comments on improving this manuscript.

## References

Acton, D.F., 1965. The relationship of patterns and gradients of slopes to soil type, *Canadian Journal of Soil Science*, 45(1): 96–101.

Asamoah, S.A., E.W. Bork, B.D. Irving, M.A. Price, and R.J. Hudson, 2003. Cattle herbage utilization patterns under high-density rotational grazing in the Aspen Parkland, *Canadian Journal of Animal Science*, 83(4):541–550.

Ayad, M.A.G., and R.L. Dix, 1964. Analysis of a vegetation micro environmental complex on prairie slopes in Saskatchewan, *Ecological Monographs*, 34(4):421–442.

Bailey, A.W., and R.A. Wroe, 1974. Aspen invasion in a portion of the Alberta parklands, *Journal of Range Management*, 27(4): 263–266.

Bolstad, P.V., and T. Stowe, 1994. An evaluation of DEM accuracy: elevation, slope, and aspect, *Photogrammetric Engineering & Remote Sensing*, 60(11):1327–1332.

Bufton, J.L., J.B. Garvin, J.F. Cavanaugh, L. Ramos-Izquierdo, T.D. Clem, and W.B. Krabill, 1991. Airborne lidar for profiling of surface topography, *Optical Engineering*, 30(1):72–78.

Campbell, C., I.D. Campbell, C.B. Blyth, and J.H. McAndrews, 1994. Bison extirpation may have caused aspen expansion in western Canada, *Ecography* 17(4):360–362.

Chang, K., and B. Tsai, 1991. The effect of DEM resolution on slope and aspect mapping, *Cartography and Geographic Information Systems*, 9(4):405–419.

Clark, M.L., D.B. Clark, and D.A. Robertsa, 2004. Small-footprint lidar estimation of sub-canopy elevation and tree height in a tropical rain forest landscape, *Remote Sensing of Environment*, 91(1):68–89.

Coupland, R.T., 1961. A reconsideration of grassland classification in the northern Great Plains of North America, *Journal of Ecology*, 49(1):135–167.

Deutsch, C.V., and A.G. Journel, 1998. *GSLIB: Geostatistical Software and User's Guide*, 2nd edition, Oxford University Press, New York, New York.

Gao, J., 1995. Comparison of sampling schemes in constructing DTMs from topographic maps, *The ITC Journal*, 1(1):18–22.

Gong, J., Z. Li, Q. Zhu, H. Sui, and Y. Zhou, 2000. Effects of various factors on the accuracy of DEMs: An intensive experimental investigation, *Photogrammetric Engineering & Remote Sensing*, 66(9):1113–1117.

Hodgson, M.E., J.R. Jensen, L. Schmidt, S. Schill, and B. Davis, 2003. An evaluation of lidar- and IFSAR-derived digital elevation models in leaf-on conditions with USGS Level 1 and Level 2 DEMs, *Remote Sensing of Environment*, 84(2): 295–308.

Hodgson, M.E., and P. Bresnahan, 2004. Accuracy of airborne Lidar-derived elevation: Empirical assessment and error budget, *Photogrammetric Engineering & Remote Sensing*, 70(3): 331–339.

Hofton, M.A., L.E. Rocchio, J.B. Blair, and R. Dubayah, 2002. Validation of Vegetation Canopy Lidar sub-canopy topography measurements for a dense tropical forest, *Journal of Geodynamics*, 34(3/4):491–502.

Jensen, J.R., 2000. *Remote Sensing of the Environment: An Earth Resource Perspective*, Prentice-Hall, New Jersey, 544 p.

Krabill, W.B., R.H. Thomas, C.F. Martin, R.N. Swift, and E.B. Frederick, 1995. Accuracy of airborne laser altimetry over the Greenland ice-sheet, *International Journal of Remote Sensing*, 16(6):1211–1222.

Leica, 2000. Leica Geosystems TC(R)702/703/705-1.1, *Open User's Manual*, pp. 39–69.

Lloyd, C.D., and P.M. Atkinson, 2002. Deriving DSMs from LiDAR data with kriging, *International Journal of Remote Sensing*, 23(12):2519–2524.

Narayanan, R.M., and B.D. Guenther, 1998. Effects of emergent grass on mid-infrared laser reflectance of soil, *Photogrammetric Engineering & Remote Sensing*, 64(5):407–413.

Ni-Meister, W., D.L.B. Jupp, and R. Dubayah, 2001. Modeling LIDAR waveforms in heterogeneous and discrete canopies, *IEEE Transactions on Geoscience and Remote Sensing*, 39(9):1943–1958.

Optech, Incorporated, 2003. About laser RADAR, Optech Incorporated, Toronto, Ontario, URL: http://www.optech.on.ca, (last date accessed: 14 August 2006).

Pereira, L., and L. Janssen, 1999. Suitability of laser data for DTM generation: A case study in the context of road planning and design, *ISPRS Journal of Photogrammetry and Remote Sensing*, 54(4):244–253.

Raber, G., 2003. The effect of LIDAR posting density on DEM accuracy and flood extent delineation, *UCGIS Summer Assembly 2003*, Asilomar Conference Grounds, 15–20 June, Pacific Grove, California.

Reutebuch, S.E., R.J. McGaughey, H.E. Andersen, and W.W. Carson, 2003. Accuracy of a high-resolution lidar terrain model under a conifer forest canopy, *Canadian Journal of Remote Sensing*, 29(5):527–535.

Scheffler, E.J., 1976. *Aspen Vegetation in a Portion of the East Central Alberta Parklands*, M.Sc. Thesis, University of Alberta, Edmonton, Alberta, Canada, 160 p.

Stelfox, J.B. (editor), 1995. *Relationship between Stand Age, Stand Structure, and Biodiversity in Aspen Mixedwood Forests in Alberta*, Jointly published by Alberta Environmental Centre (AECV95-R1), Vegreville, Alberta, and Canadian Forest Service (Project No. 0001A), Edmonton, Alberta, Canada.

Strong, W.L., 1992. *Ecoregions and Ecodistricts of Alberta*, Alberta Forestry, Lands and Wildlife, Land Information Services Division, Edmonton, Alberta, Publication T/244.

Su, G., 2004. *DEM Modeling, Vegetation Characterization and Mapping of Aspen Parkland Rangeland Using lidar Data*, Ph.D. Thesis, University of Alberta, Edmonton, Alberta, Canada. 159 p.

Thomas, L., and F. Juanes, 1996. The importance of statistical power analysis: An example from Animal Behaviour, *Animal Behaviour*, 52(4):856–859.

Trottier, G.C., 1986. Disruption of rough fescue, Festuca hallii, grassland by livestock grazing in Riding Mountain National Park, Manitoba, *Canadian Field Naturalist*, 100(3):488–495.

Tsutsui, K., K. Koya, and T. Kato, 1998. An investigation of continuous-angle laser light scattering, *Review of Scientific Instruments*, 69(10):3482–3486.

Walker, B.H., and R.T. Coupland, 1970. Herbaceous wetland vegetation in the aspen grove and grassland region of Saskatchewan, *Canadian Journal of Botany*, 48(9):1861–1878.

Weltz, M.A., J.C. Ritchie, and H.D. Fox, 1994. Comparison of laser and field measurements of vegetation heights and canopy cover, *Water Resources Research*, 30(5):1311–1320.

Wheeler, G.W., 1976. *Some Grassland and Shrubland Communities in the Parklands of Central Alberta*, M.Sc. Thesis, University of Alberta, Edmonton, Alberta, Canada. 95 p.

Wright, H.A., and A.W. Bailey, 1982. *Fire Ecology: United States and Southern Canada*, John Wiley & Sons, New York, New York.

(Received 29 November 2004; accepted 13 June 2005; revised 06 September 2005)